NACA

RESEARCH MEMORANDUM

A BRIEF ANALOG INVESTIGATION OF INERTIA COUPLING IN ROLLING MANEUVERS OF AN AIRPLANE CONFIGURATION USING A VARIABLE-INCIDENCE WING AS THE LONGITUDINAL CONTROL

By Clarence L. Gillis

Langley Aeronautical Laboratory
Langley Field, Va.

NATIONAL ADVISORY COMMITTEE
FOR AERONAUTICS

WASHINGTON

August 6, 1957
Declassified September 29, 1959

NACA RM L57F18

NATIONAL ADVISORY COMMITTEE FOR AERONAUTICS

RESEARCH MEMORANDUM

A BRIEF ANALOG INVESTIGATION OF INERTIA COUPLING IN ROLLING MANEUVERS OF AN AIRPLANE CONFIGURATION USING A VARIABLE-INCIDENCE WING AS THE LONGITUDINAL CONTROL

By Clarence L. Gillis

SUMMARY

An analog computer study was made in order to investigate the inertia coupling in rolling maneuvers of an airplane configuration utilizing a variable-incidence wing for longitudinal control. A five-degree-of-freedom system of equations was used, and only one set of flight conditions was included in this study. The results, when compared to those for a conventional tail-control airplane, indicated significant advantages for the variable-incidence-wing type of control in reducing undesired dynamic effects during rolling maneuvers.

INTRODUCTION

The problem of inertia coupling of the longitudinal and lateral motions of airplanes in rolling maneuvers has been extensively investigated, both experimentally and analytically, and various methods have been proposed for eliminating roll coupling or at least reducing the magnitude of the coupling to acceptable values. (See refs. 1 to 7.) Reference 7 contains a good discussion of the effects of the individual coupling terms and of the interaction of these coupling terms to produce the complex dynamic response during rolling maneuvers. The investigation described herein concerns a proposed method of operation of airplanes which might lead to reduced inertia coupling as well as to some other possible advantages. The method of operation consists of obtaining normal acceleration by varying the wing incidence while keeping the fuselage at a relatively constant angle of attack, as is done for some missiles. Other studies (refs. 3 and 7) have shown that one of the most important effects causing coupled longitudinal and lateral motions is a term in the side-force equation proportional to the product of angle of attack

and rolling velocity. By permitting the fuselage, and thus the principal axis, to remain at a small and relatively constant angle of attack, the variable-incidence-wing type of longitudinal control might thus alleviate the inertia coupling problem.

The present investigation is preliminary because the investigation considers only one configuration, which may not be optimum as far as variable-incidence operation is concerned, and because the calculations are made for only one set of flight conditions and for one type of rolling-pullout maneuver. Calculations to simulate airplane motions were made on an electronic analog computer at the Langley Aeronautical Laboratory, using a five-degree-of-freedom system of equations, with forward velocity considered constant. The flight conditions and mass characteristics used for the calculations represented a free-flight rocket-propelled model airplane. The application of results to a full-scale airplane is discussed.

SYMBOLS

C_L	lift coefficient, $\frac{\text{Lift}}{q'S}$
C_m	pitching-moment coefficient, $\frac{\text{Pitching moment}}{q'S\bar{c}}$
C_l	rolling-moment coefficient, $\frac{\text{Rolling moment}}{q'Sb}$
C_n	yawing-moment coefficient, $\frac{\text{Yawing moment}}{q'Sb}$
C_Y	lateral-force coefficient, $\frac{\text{Lateral force}}{q'S}$
b	wing span, ft
$\bar{c}$	wing mean aerodynamic chord, ft
I_X, I_Y, I_Z	moments of inertia about X-, Y-, and Z-axes (fig. 1), slug-ft^2
I_{XZ}	product of inertia
k_X, k_Y, k_Z	radii of gyration about X-, Y-, and Z-axes, ft

M	Mach number
m	mass, slugs
p	rolling angular velocity, radians/sec
p_∞	atmospheric pressure, lb/sq ft
q	pitching angular velocity, radians/sec
q'	dynamic pressure, lb/sq ft
r	yawing velocity, radians/sec
S	wing area, sq ft
t	time, sec
V	velocity, ft/sec
W	weight, lb
α	angle of attack, radians
β	angle of sideslip, radians
δ	longitudinal control deflection (positive with trailing edge down), radians
δ_a	differential deflection of two ailerons (positive in a direction to give positive roll), radians
ρ	atmospheric density, slug/cu ft
μ	relative density factor, $m/\rho S\bar{c}$

Subscripts:

max	maximum
s	stabilizer
ss	steady state
w	wing
c	conventional configuration
v	variable-incidence-wing configuration

The quantities α, β, δ, and δ_a used as subscripts to coefficients indicate the partial derivative of the coefficient with respect to the quantity, such as

$$C_{L_\alpha} = \frac{\partial C_L}{\partial \alpha}$$

The quantities $\dot{\alpha}$, $\dot{\beta}$, p, q, and r used as subscripts to coefficients indicate the partial derivative of the coefficient with respect to the nondimensional quantities $\dot{\alpha}\bar{c}/2V$, $\dot{\beta}b/2V$, $pb/2V$, $q\bar{c}/2V$, and $rb/2V$ such as

$$C_{m_{\dot{\alpha}}} = \frac{\partial C_m}{\partial\left(\frac{\dot{\alpha}\bar{c}}{2V}\right)} \quad \text{and} \quad C_{l_p} = \frac{\partial C_l}{\partial\left(\frac{pb}{2V}\right)}$$

EQUATIONS OF MOTION

The equations of motion were written for the body axes system illustrated in figure 1. These axes are considered fixed in the fuselage for all calculations presented herein. The equations as set up for the analog computer were

$$\dot{\alpha} = q - \beta p - \frac{q'S}{mV}\left(C_{L_\alpha}\alpha + C_{L_\delta}\delta\right) \tag{1}$$

$$\dot{\beta} = -r + \alpha p + \frac{q'S}{mV} C_{Y_\beta}\beta \tag{2}$$

$$\dot{p} = \frac{I_Y - I_Z}{I_X} qr + \frac{I_{XZ}}{I_X}\left(\dot{r} + pq\right) + \frac{q'Sb}{I_X}\left(C_{l_{\delta_a}}\delta_a + C_{l_\beta}\beta\right) + \frac{q'Sb^2}{2VI_X}\left(C_{l_p}p + C_{l_r}r\right) \tag{3}$$

$$\dot{q} = \frac{I_Z - I_X}{I_Y} pr + \frac{I_{XZ}}{I_Y}\left(r^2 - p^2\right) + \frac{q'S\bar{c}^2}{2VI_Y}\left(C_{m_q}q + C_{m_{\dot{\alpha}}}\dot{\alpha}\right) + \frac{q'S\bar{c}}{I_Y}\left(C_{m_\alpha}\alpha + C_{m_\delta}\delta\right) \tag{4}$$

$$\dot{r} = \frac{I_X - I_Y}{I_Z} pq + \frac{I_{XZ}}{I_Z}\left(\dot{p} - qr\right) + \frac{q'Sb}{I_Z}\left(C_{n_\beta}\beta + C_{n_{\delta_a}}\delta_a\right) +$$

$$\frac{q'Sb^2}{2VI_Z}\left(C_{n_r}r + C_{n_{\dot{\beta}}}\dot{\beta} + C_{n_p}p\right) \qquad (5)$$

All gravity terms have been omitted from the above equations as well as certain aerodynamic terms such as $C_m(\beta)$ and C_{Y_r}. For the flight conditions used herein the gravity terms are small and approximately equal for the two configurations, and the aerodynamic terms omitted are assumed to be negligible. In the calculations it was assumed that $\dot{\beta} = -r$ in equation (5), thus a slight simplification of the last term is possible.

CALCULATIONS

The calculations were made for the configuration shown in figure 2. This configuration was chosen from considerations of expediency, and no studies were made to derive an optimum configuration when a variable-incidence wing was employed. Aerodynamic data on this and a similar configuration were available from references 8 and 9.

The calculations were made for a Mach number of 2.0. The flight conditions used were those existing on the rocket-powered model of reference 8 at this Mach number. These conditions, at low altitudes (see table I), are dynamically similar to a representative full-scale airplane at altitudes in the range of 30,000 to 50,000 feet, as is discussed in the section on "Application to Full-Scale Airplane."

Calculations were made for both a conventional configuration, that is, a configuration with a fixed wing and an all-movable stabilizer, and for a configuration with an all-movable wing and a fixed stabilizer. The aerodynamic characteristics used for the two configurations are given in table II. In estimating C_{L_δ} and C_{m_δ} for the variable-incidence-wing airplane the loss in lift across the fuselage and the effect of the downwash on the tail from the deflected wing were accounted for. No changes in the derivatives with angle of attack were considered. The calculations included two values of C_{l_β}, as indicated in table II.

In order to keep the fuselage at a relatively fixed angle of attack during maneuvers, the term C_{m_δ} for the variable-incidence wing control ideally must be zero. For any given set of flight conditions C_{m_δ} can

usually be kept at zero by making fairly small changes in configuration; for example, in the present case C_{m_δ} can be made zero while keeping C_{m_α} the same as for the conventional configuration by moving the wing forward 7 percent of the mean aerodynamic chord and approximately doubling the horizontal-tail area, as indicated by the dotted lines in figure 2. Further comments on this subject are included subsequently.

The maneuver chosen for the calculations was a pull-up followed by a roll. The airplane was assumed to be in level flight initially, and an abrupt stabilizer or wing deflection was applied to produce a change in steady-state lift coefficient of 0.2. Aileron deflections were then applied at two different times during the maneuver. In one set of runs the transient motion resulting from the pull-up was allowed to damp to a small magnitude, and the aileron deflection was then applied abruptly. In the other set of runs the aileron deflection was applied abruptly at or near the first peak in normal acceleration (or angle of attack) following the control motion. In both cases the ailerons remained deflected for a time interval sufficient to give approximately a 150° to 180° roll. The ailerons were then moved abruptly back to neutral, and following another time interval to permit damping of the resulting transient the stabilizer was also returned to neutral. Some studies have indicated that larger transient motions may be encountered in recovering from a maneuver than during the maneuver. Several different aileron deflections were used to produce rolling velocities from low values up to values near those corresponding to resonance with the yawing motion (20 radians/sec). The natural frequency in pitch was 23 radians/second. The rolling divergence at resonance was not investigated in this study. Almost all of the operational rolling motions of an airplane occur at roll rates less than the resonance rate, and even under these conditions severe excursions in pitch and yaw can occur and lead to violent motions and excessive aircraft loads (ref. 4). Calculations for the variable-incidence-wing airplane included several other conditions, but these conditions are more conveniently discussed with the results where their purpose becomes clear.

RESULTS

A total of about 60 analog computer runs were made. For illustrative purposes 23 of these runs are shown in figures 3 to 7 as time histories of lateral and longitudinal motions. Summary plots of some of the significant results are presented in figures 8 to 10.

DISCUSSION

Longitudinal Motion

Pure longitudinal motion, with no aileron deflection, is shown in figure 3 for both the conventional and variable-incidence configuration. During the pull-up the steady-state value of pitching velocity is the same for the two configurations, as it should be, because a lift coefficient increment of 0.2 was called for during the maneuver. The change in steady-state angle of attack is about 7° for the conventional configuration and very nearly 0° when the variable-incidence wing is used. The amplitude of the oscillatory motion resulting from abrupt deflection of the control is much smaller for the variable-incidence-wing configuration.

Combined Motions

Some preliminary computer runs indicated that for the variable-incidence configuration the steady rolling velocity was appreciably higher than for the conventional configuration with the same aileron deflection. Since a comparison of the two configurations on the basis of equal rolling velocities rather than equal aileron deflections is more meaningful for a study of the motions, the aileron deflections for the variable-incidence configuration were reduced for almost all of the runs so as to produce rolling velocities more nearly equal to those for the conventional configuration.

Time histories.- For the combined longitudinal and lateral motions the majority of the calculations were performed with $C_{l_\beta} = -0.10$, which corresponds to the airplane with no wing dihedral. These results are presented in figures 4 and 5. The aileron deflections were chosen so that the largest values used would give roll velocities near the uncoupled yaw frequency (20 radians/sec), according to an estimate from an equation for a single-degree-of-freedom roll. For the conventional configuration with $C_{l_\beta} = -0.10$ the rolling velocities are only about one-half of those from the single-degree-of-freedom calculations. This result is primarily due to positive sideslip angles, developed during the maneuvers (fig. 4), which produce opposite rolling moments because of the dihedral effect. These positive sideslip angles are caused by coupling terms other than aerodynamic since $C_{n_{\delta_a}}$ and C_{n_p} were assumed to be zero for all calculations herein. (See table II.) Coupling effects on the longitudinal motion of the conventional configuration are evident in figures 4(b), (c), and (d) by increases in magnitude of q and α during the time the aileron is deflected. When the aileron

deflection was applied near the first peak in angle of attack (fig. 5) the lateral motions of the conventional configuration were more violent, with the rolling velocity reversing sign for a short time in one case (fig. 5(a)).

The first calculations with the variable-incidence wing were made with the fuselage steady-state angle of attack equal to zero. These calculations indicated oscillatory instability for the smallest aileron deflection (dotted line, fig. 4(a)) and divergence for the larger aileron deflections (dotted lines, figs. 4(b) and 5(a)). The aileron deflections for these runs were the same as for the conventional configuration, and the higher rolling velocity is evident in figure 4(a). It is not believed that the larger rolling velocities are the cause of the instability, however, because as shown later higher rolling velocities were obtained on other runs without producing instability. Since for the condition of zero fuselage angle of attack the airplane principal axis is inclined nose down with respect to the flight path, it appeared that poor damping of the lateral motion may have been the basic cause of the unsatisfactory motion and that only a small amount of coupling produced instability. Note in figure 4(a) that the oscillatory lateral motion, which is excited by the aileron deflection and then increases in amplitude, subsequently damps when the wing deflection is returned to zero.

In order to obtain better damping of the lateral oscillations the fuselage can be trimmed to some positive angle of attack rather than zero, as in the first variable-incidence calculations. A constant deflection of the horizontal tail will accomplish this trimming; accordingly, two additional sets of calculations were made with the fuselage angle of attack at 1/3 and 2/3, respectively, of the value of the angle of attack of the conventional configuration during the pull-up at a lift coefficient of 0.2. Both sets of calculations showed damped motions with no divergences, and there was little difference between the two sets; therefore, all motions subsequently discussed for the variable-incidence-wing configuration are for the condition of the fuselage steady-state angle of attack equal to 1/3 of that for the conventional configuration during the pull-up.

The importance to the coupled motion of the αp term in the side-force equation can be seen by observing the effect of the steady-state angle of attack on the initial sideslip transients in figures 4(a), 4(b), and 5(a). A decrease in angle of attack from 0.12 radian (6.9°) for the conventional configuration to 0.04 radian (2.3°) for the variable incidence configuration resulted in large reductions in the initial sideslip angles. A further decrease in angle of attack to zero caused a reversal in sign of the initial sideslip motions. The angle of attack of the principal axis is negative for the latter case. In figures 4(b) and 4(a) it is evident that for the zero angle-of-attack case the positive rolling velocity and negative sideslip angle are reinforcing each

other to the extent that apparent divergences in both the lateral and longitudinal motions existed.

Although the aileron deflections for the variable-incidence configuration with a positive trim angle of attack are about 25 percent smaller than for the conventional configuration, the rolling velocities are slightly higher (figs. 4 and 5) because of the smaller sideslip angles developed by the variable-incidence configuration during rolling. The yawing velocities during the roll are considerably smaller for the variable-incidence airplane.

For the cases with aileron applied near the first peak in angle of attack (fig. 5) the variations in rolling velocity and sideslip angle were much less for the variable-incidence configuration (long dash line, fig. 5) than for the conventional configuration (solid line, fig. 5). No reversals in direction occurred for the variable-incidence configuration prior to return of the aileron to neutral. Effects of the lateral motion on the longitudinal motion are evident in figures 4 and 5 for the variable-incidence configuration, but in no case do these effects appear to be larger than for the conventional configuration.

For the motions in figures 4(a), 4(c), and 5(b) the amplitudes of the lateral oscillations remaining after the ailerons are returned to neutral are larger for the variable-incidence configuration than for the conventional configuration, while for all other motions illustrated the opposite is true. The effect seemed to occur randomly in about 1/4 to 1/3 of the comparable analog runs made for the two configurations and is probably a function of the initial conditions existing when the ailerons are returned to neutral.

The large losses in rolling velocity caused by the sideslip angles indicated that in terms of airplane flying qualtities the effective dihedral of the airplane was excessive for the calculations previously discussed. Additional calculations were made with C_{l_β} reduced to -0.02, as might be obtained with negative wing dihedral, and some of these results are presented in figures 6 and 7. Note that the β scale in figures 6 and 7 has been reduced by a factor of five from that used in previous figures.

The conclusions obtained from the study of motions with $C_{l_\beta} = -0.10$ are even more strongly evident from the motions with $C_{l_\beta} = -0.02$. For a given aileron deflection smaller losses in rolling velocity caused by sideslip angles occurred when C_{l_β} was reduced. The variable-incidence airplane again produced higher rolling velocities than the conventional configuration for the same aileron deflection. With the dihedral reduced the variable-incidence airplane had an even greater advantage over the

conventional airplane and produced maximum sideslip angles only about 1/5 as large. The yawing velocities were again much smaller for the variable-incidence airplane than for the conventional.

Summary plots.- Some of the results of this investigation are summarized in figures 8 to 10. Figure 8 shows the approximate steady-state rolling velocities obtained compared with those that would be obtained from a single-degree-of-freedom roll. The large losses in rolling velocity due to the sideslip developed are evident. For the same aileron deflections the rolling velocities for the variable-incidence configuration were higher than for the conventional configuration by about 50 percent for $C_{l_\beta} = -0.10$ and by about 30 percent for $C_{l_\beta} = -0.02$.

The values of maximum sideslip angle shown in figure 9 are significantly less for the variable-incidence configuration than for the conventional configuration at the same rolling velocity. Although the resonance condition was not reached it was closely approached and figure 9(b) shows that for the conventional configuration the sideslip angle excursions were increasing at a rapid rate at the higher rolling velocities. The rate of increase with rolling velocity for the variable-incidence configuration was much smaller.

The large reductions in maximum yawing velocity produced by the variable-incidence airplane compared with the conventional are illustrated in figure 10. The maximum yawing velocities were not as greatly affected by reducing the dihedral as were the maximum sideslip angles.

Inertia coupling terms.- The terms in the equations listed previously which cause coupling of the lateral and longitudinal motions are terms proportional to βp, αp, qr, pq, pr, r^2, and p^2. For the airplane configuration and flight conditions used in the calculations herein, the results indicated that for equal rolling velocities the quantities β, α, r, and the transient portion of q were smaller for the variable-incidence-wing type of pitch control than for conventional tail control. While p^2 and the steady-state values of pq were the same for the two modes of operation, all other coupling terms were smaller for the variable-incidence configuration. This fact was confirmed by recorded values of some of these coupling terms obtained but not illustrated herein. For a rolling maneuver during a steady pull-up (q = constant) the term pq will be the same regardless of the type of control used or of the airplane attitude (except insofar as p is affected by the choice of axes). By referring to equation (5) it can be seen that if q is constant the term $\frac{I_X - I_Y}{I_Z} pq$ produces an effective negative value of C_{n_p} for the type of airplane under consideration

(I_Y larger than I_X), as pointed out in reference 3. Negative values of C_{n_p} produce destabilizing effects on the lateral motion (refs. 3 and 10). Because significant reduction in β and r was obtained when the variable-incidence wing was used, the conclusion is reached that the destabilizing effect of the pq term was small when compared with the beneficial reductions in other coupling terms such as αp.

Application to Full-Scale Airplane

As mentioned previously, the flight conditions used in this investigation were those existing at a Mach number of 2.0 for the rocket-propelled airplane model of reference 8. The motions obtained in this study, when nondimensionalized to the forms $pb/2V$, $q\bar{c}/2V$, and $rb/2V$, can be considered as applying to a full-scale airplane having dynamic similarity; that is, the same value of the relative density factor μ and the same nondimensional radii of gyration such as k_X/b and $k_Y/\bar{c}$. For example, if the model used is assumed to be a 1/6-scale model of a 25,000-pound airplane, then the equivalent airplane altitude is about 40,000 feet. The results in figures 3 to 10 may be considered to apply directly to such an airplane if the values of the scales for angular velocities are divided by 6.56 and the values of the time scale are multiplied by the same factor since this factor accounts for the airplane-to-model scale ratio and the variation of speed of sound with altitude.

For the present investigation the value of C_{m_α} for the variable-incidence-wing configuration was kept the same as for the conventional configuration so that the natural frequencies in pitch, which appear in frequency ratios that are important in roll coupling (ref. 1), would be the same. For a conventional airplane the static stability C_{m_α} provides stability of the short-period motion and acts as a spring constant which must be overcome by the longitudinal control C_{m_δ} in order to maneuver the airplane. For a variable-incidence airplane the latter function disappears, and the criterion for establishing desirable values of static stability may be quite different. For example, greater freedom might be possible for selecting the pitch frequency in relation to the yaw frequency and thus further reduce the coupling tendencies.

The condition $C_{m_\delta} = 0$ may be satisfied for any given set of flight conditions by the proper choice of size and location of wing and tail, as indicated previously. It is not to be expected that C_{m_δ} will remain zero as the Mach number and altitude change. The value of C_{m_δ} might be kept relatively small, however, by suitable choice of tail plan form and aspect ratio. The effect of such nonzero values of C_{m_δ} on the coupled

motions would, of course, be an important factor for investigation when assessing the value of variable-incidence-wing control.

CONCLUDING REMARKS

The brief investigation described herein indicates that the use of a variable-incidence wing as the primary longitudinal control for airplanes may offer some advantages over a conventional tail control in the matter of reducing undesired dynamic effects during pullout rolling maneuvers. Some of these advantages are: smaller pitch transients during a symmetrical pull-up; greater rolling velocity for a given aileron deflection because of smaller adverse sideslip angles; and a reduction in inertia coupling between longitudinal and lateral motions. It was indicated that one of the primary effects leading to the reduced coupling was the small fuselage angles of attack permitted by the variable-wing-incidence type of control. The present study is limited in that only one set of flight conditions was used in the study, and no attempt to derive the optimum variable-incidence configuration was made. It is believed, however, that this investigation indicates sufficient promise of benefit to be derived from the use of a variable-incidence wing that further investigation is warranted.

Langley Aeronautical Laboratory,
National Advisory Committee for Aeronautics,
Langley Field, Va., June 5, 1957.

REFERENCES

1. Phillips, William H.: Effect of Steady Rolling on Longitudinal and Directional Stability. NACA TN 1627, 1948.

2. Weil, Joseph, Gates, Ordway B., Jr., Banner, Richard D., and Kuhl, Albert E.: Flight Experience of Inertia Coupling in Rolling Maneuvers. NACA RM H55E17b, 1955.

3. Stone, Ralph W., Jr.: An Analytical Study of Sideslip Angles and Vertical-Tail Loads in Rolling Pullouts As Affected by Some Characteristics of Modern High-Speed Airplane Configurations. NACA RM L53G21, 1953.

4. Sternfield, Leonard: A Simplified Method for Approximating the Transient Motion in Angles of Attack and Sideslip During a Constant Rolling Maneuver. NACA RM L56F04, 1956.

5. Gates, Ordway B., Jr., Weil, Joseph, and Woodling, C. H.: Effect of Automatic Stabilization on the Sideslip and Angle-of-Attack Disturbances in Rolling Maneuvers. NACA RM L55E25b, 1955.

6. Phillips, William H.: Analysis of an Automatic Control To Prevent Rolling Divergence. NACA RM L56A04, 1956.

7. Welch, J. D., and Wilson, R. E.: Cross Coupling Dynamics and the Problems of Automatic Control in Rapid Rolls. Preprint No. 691, S.M.F. Fund Preprint, Inst. Aero. Sci., Jan. 1957.

8. Peck, Robert F.: Results of Rocket Model Test of an Airplane Configuration Having an Arrow Wing and Slender Flat-Sided Fuselage. Lift, Drag, Longitudinal Stability, Lateral Force, and Jet Effects at Mach Numbers Between 1.0 and 2.3. NACA RM L55L29, 1956.

9. Margolis, Kenneth, and Bobbitt, Percy J.: Theoretical Calculations of the Stability Derivatives at Supersonic Speeds for a High-Speed Airplane Configuration. NACA RM L53G17, 1953.

10. Gates, Ordway B., Jr., and Woodling, C. H.: A Method for Estimating Variations in the Roots of the Lateral-Stability Quartic Due to Changes in Mass and Aerodynamic Parameters of an Airplane. NACA TN 3134, 1954.

TABLE I

FLIGHT CONDITIONS AND MASS CHARACTERISTICS

M	2.0
V, ft/sec	2,200
q', lb/sq ft	3,760
p_∞, lb/sq ft	1,347
W, lb	300
I_X, slug-ft^2	3.7
I_Y, slug-ft^2	102
I_Z, slug-ft^2	104
I_{XZ}, slug-ft^2	4

TABLE II

AERODYNAMIC CHARACTERISTICS

	Conventional	Variable incidence
C_{L_α}	2.0	2.0
C_{L_δ}	0.12	1.5
C_{m_α}	-0.60	-0.60
C_{m_δ}	-0.25	0
C_{m_q}	-1.10	-1.10
$C_{m_{\dot{\alpha}}}$	-0.55	-0.55
C_{Y_β}	-0.75	-0.75
C_{l_β}	-0.10 -0.02	-0.10 -0.02
$C_{l_{\delta_a}}$	0.01	0.01
C_{l_p}	-0.15	-0.15
C_{l_r}	0.1	0.1
C_{n_β}	0.2	0.2
$C_{n_r} - C_{n_{\dot{\beta}}}$	-2.0	-2.0
$C_{n_{\delta_a}}$	0	0
C_{n_p}	0	0

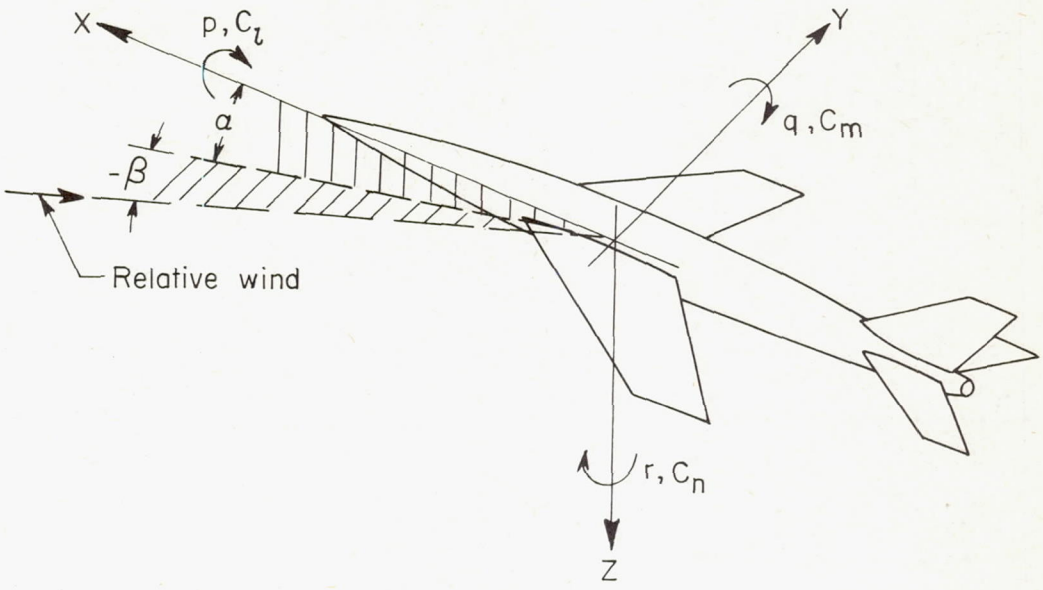

Figure 1.- Body-axes system. All quantities illustrated in positive direction except β.

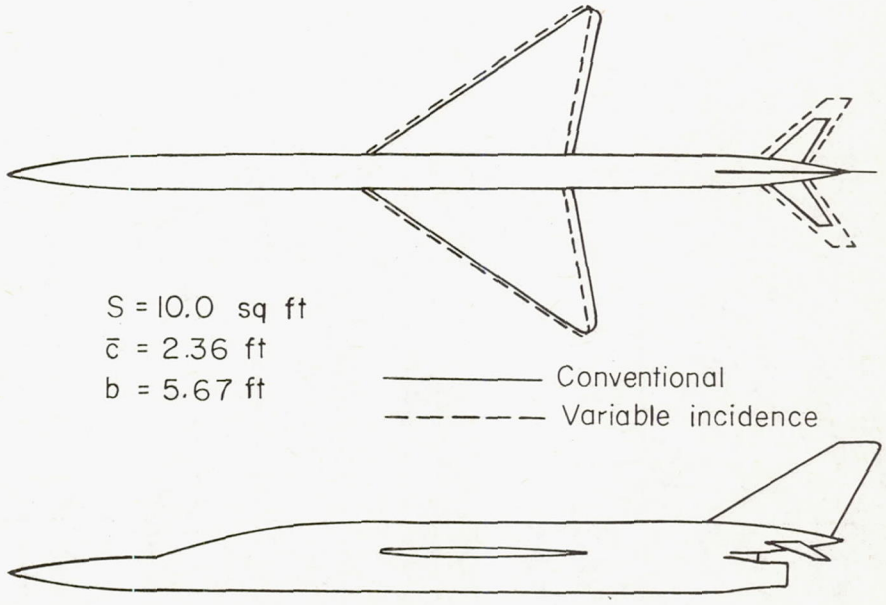

Figure 2.- Airplane configuration used in study.

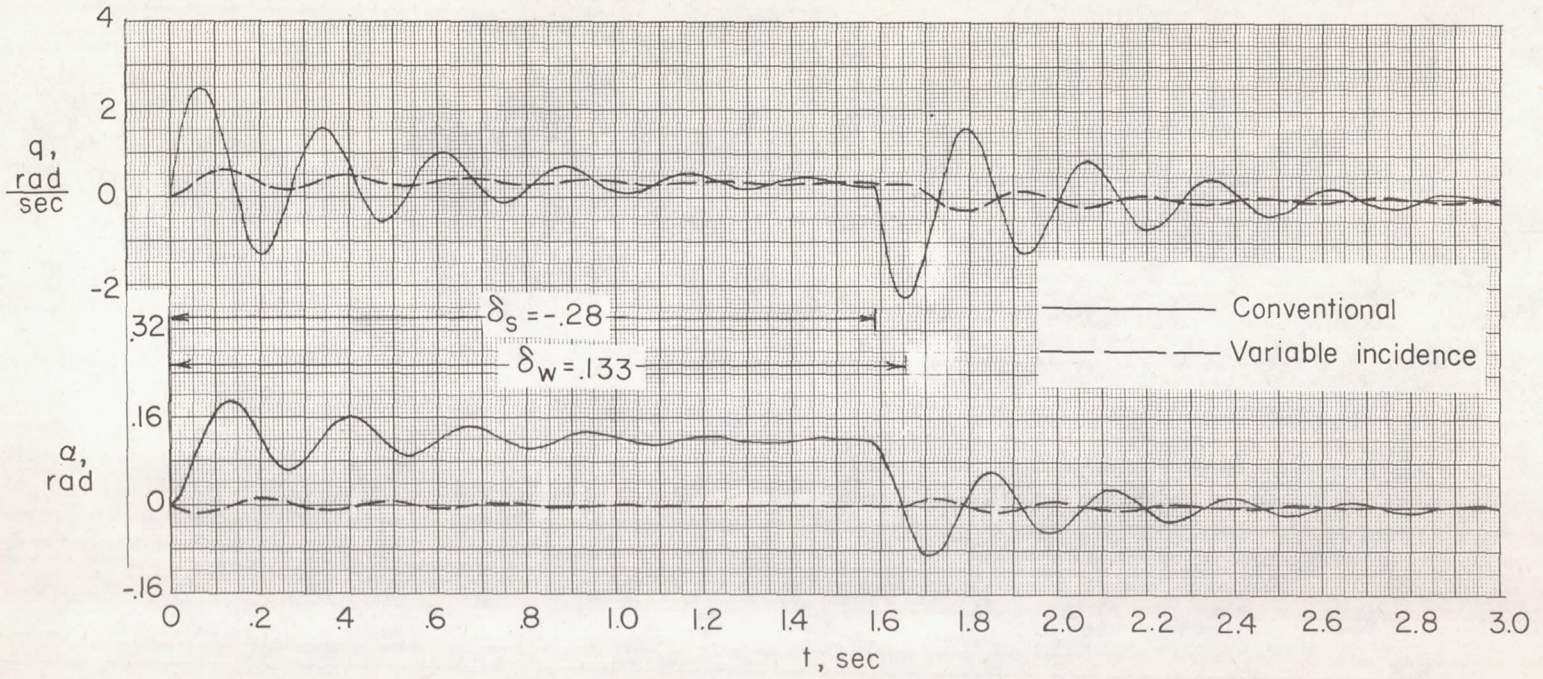

Figure 3.- Longitudinal response to pitch control deflection.

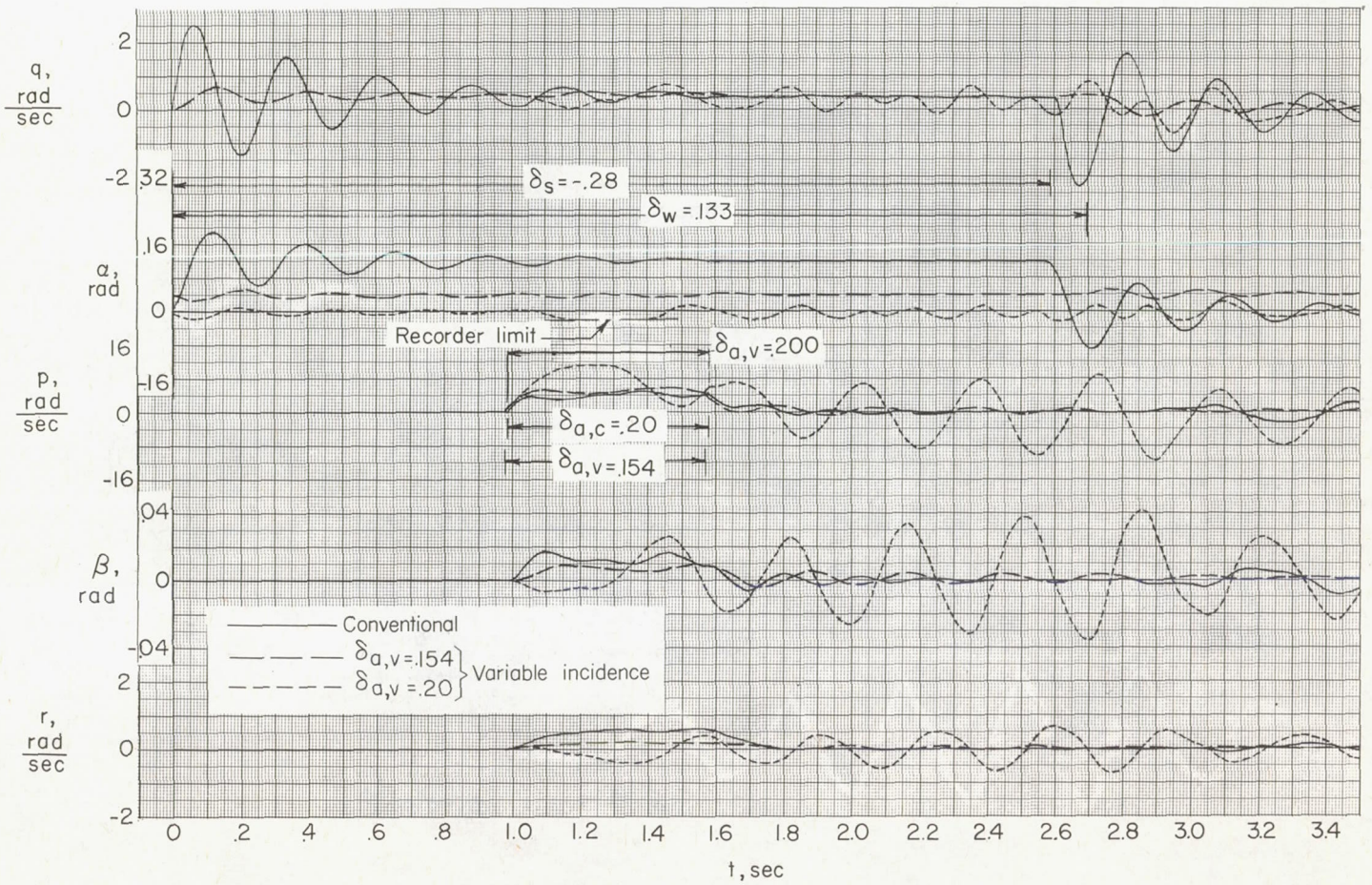

(a) $\delta_{a,c} = 0.200$; $\delta_{a,v} = 0.154$ and 0.200.

Figure 4.- Combined lateral and longitudinal motions. Aileron deflection applied at 1.0 sec. $C_{l_\beta} = -0.10$.

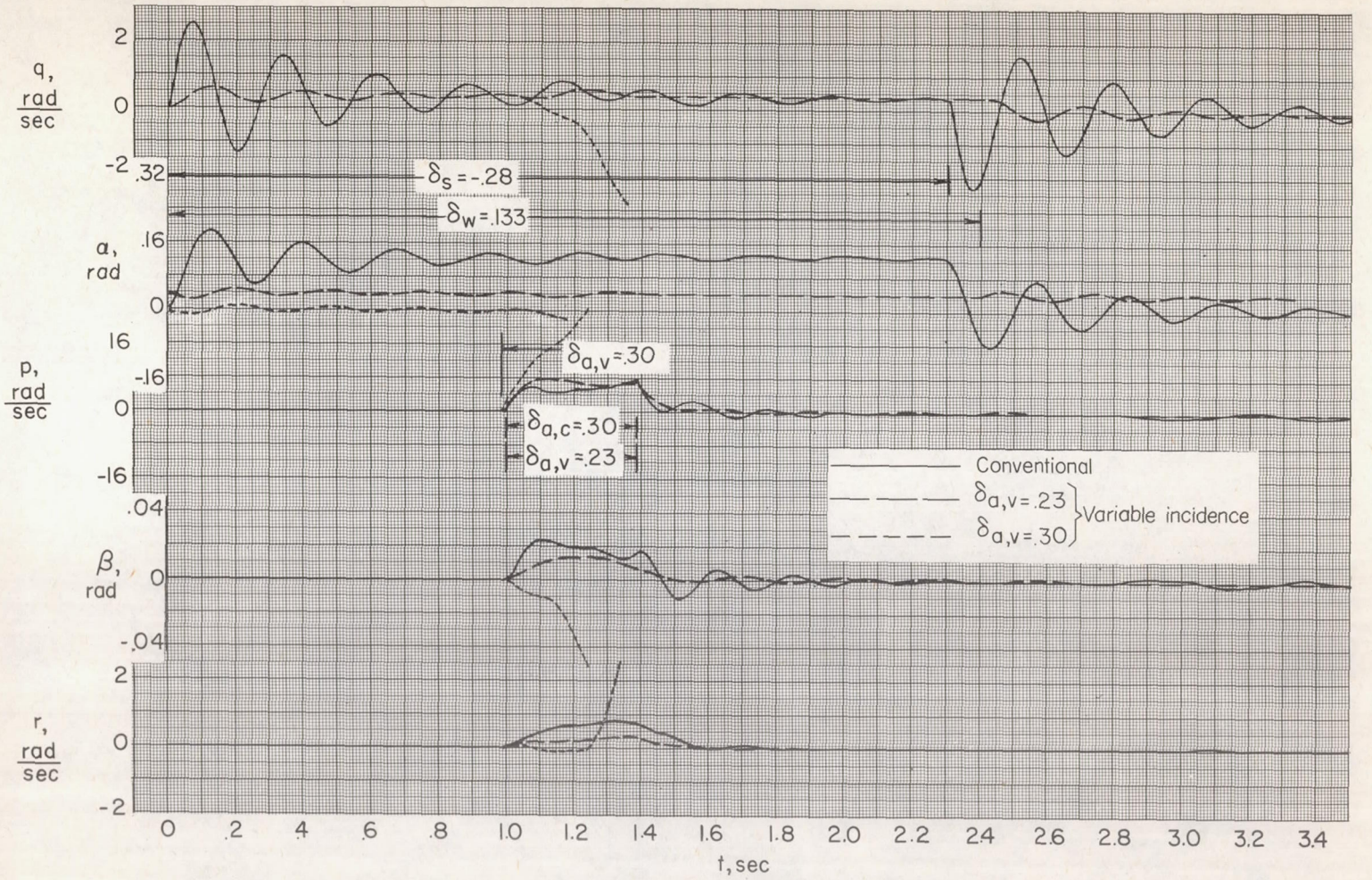

(b) $\delta_{a,c} = 0.300$; $\delta_{a,v} = 0.230$ and 0.300.

Figure 4.- Continued.

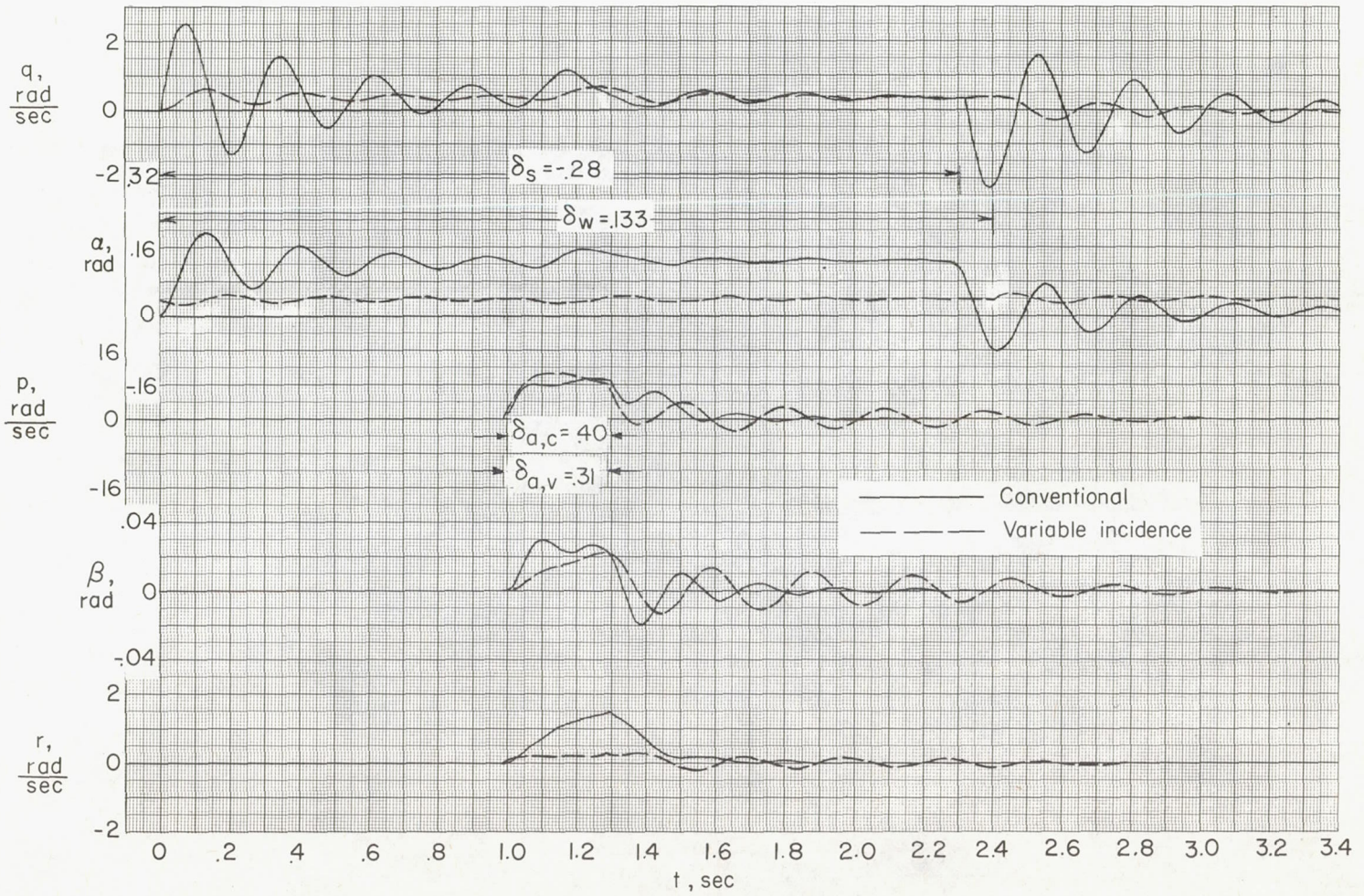

(c) $\delta_{a,c} = 0.400$; $\delta_{a,v} = 0.310$.

Figure 4.- Continued.

(d) $\delta_{a,c} = 0.500$; $\delta_{a,v} = 0.390$.

Figure 4.- Concluded.

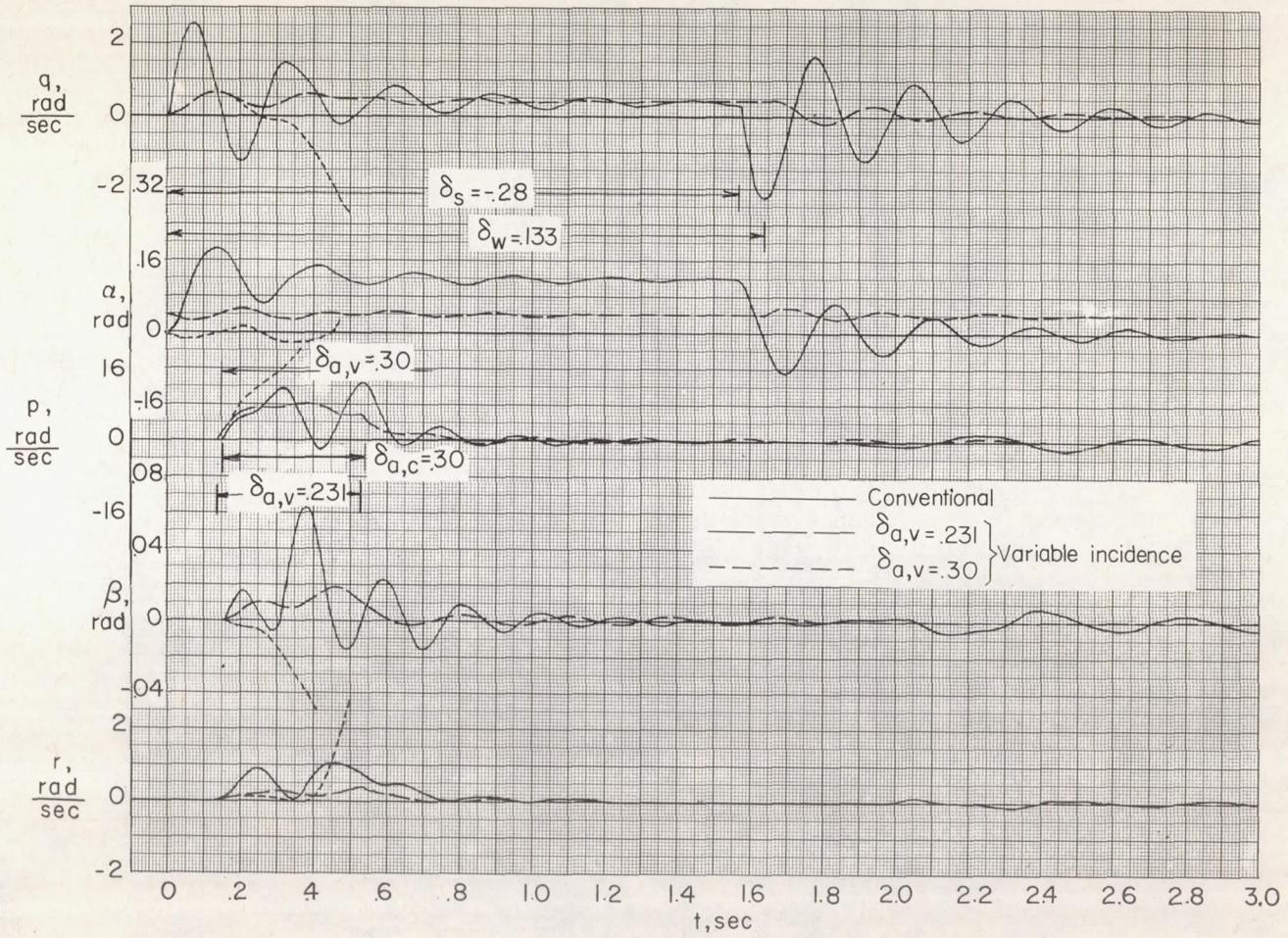

(a) $\delta_{a,c} = 0.300$; $\delta_{a,v} = 0.231$ and 0.300.

Figure 5.- Combined lateral and longitudinal motions. Aileron deflection applied after one-fourth cycle of pitch oscillation. $C_{l_\beta} = -0.10$.

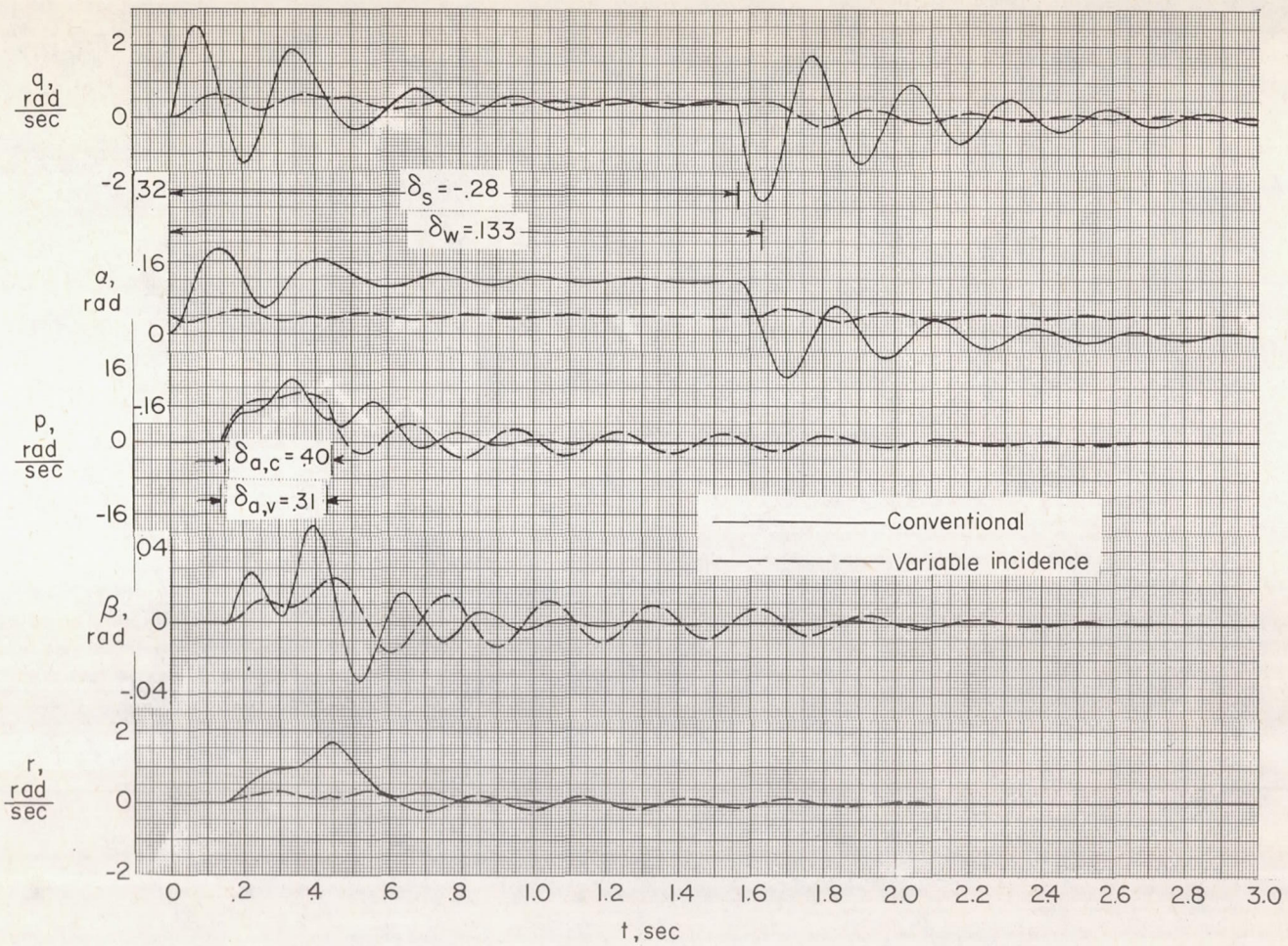

(b) $\delta_{a,c} = 0.400$; $\delta_{a,v} = 0.310$.

Figure 5.- Concluded.

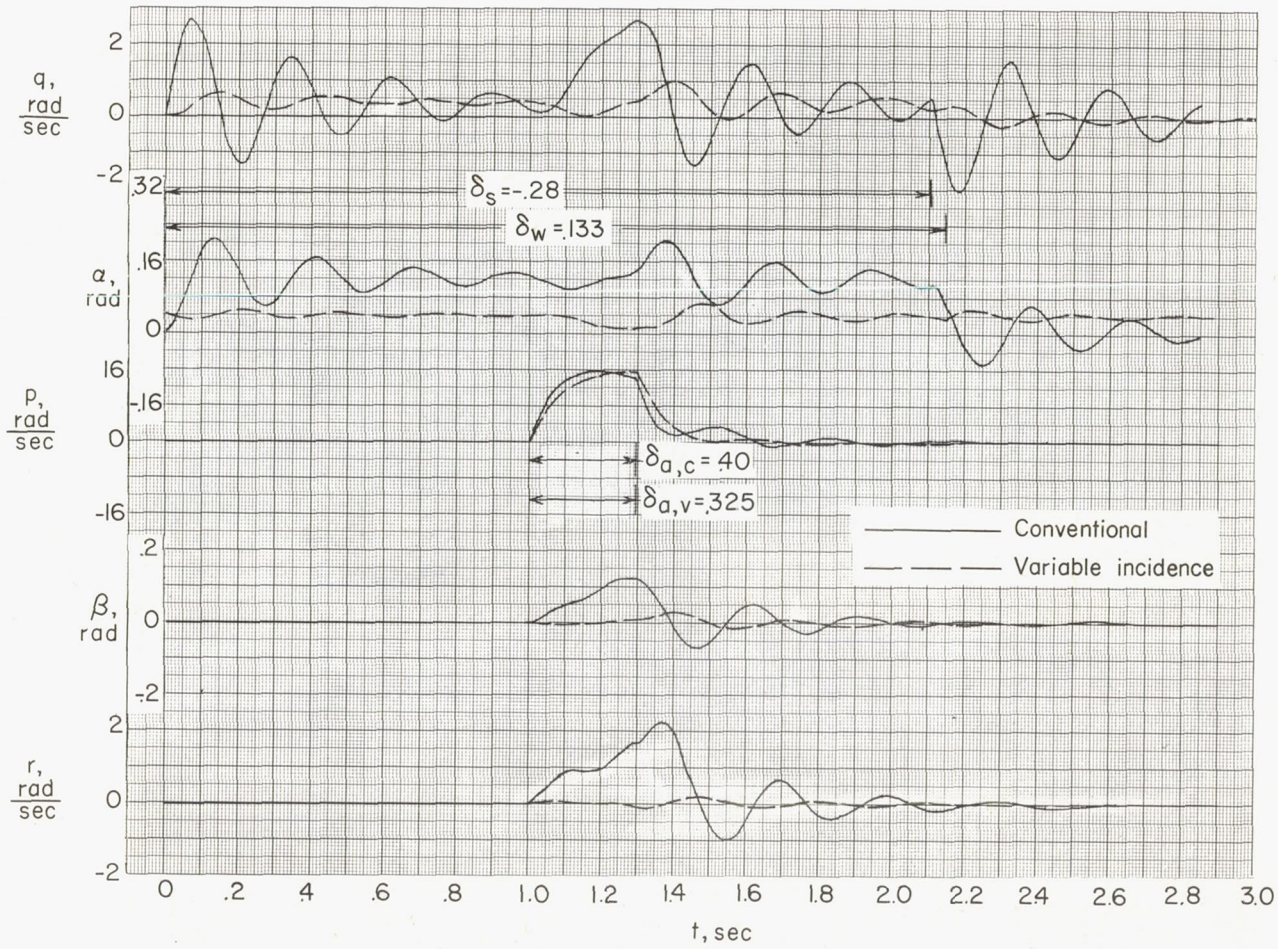

(a) $\delta_{a,c} = 0.400$; $\delta_{a,v} = 0.325$.

Figure 6.- Combined lateral and longitudinal motions. Aileron deflection applied at 1.0 sec. $C_{l_\beta} = -0.02$.

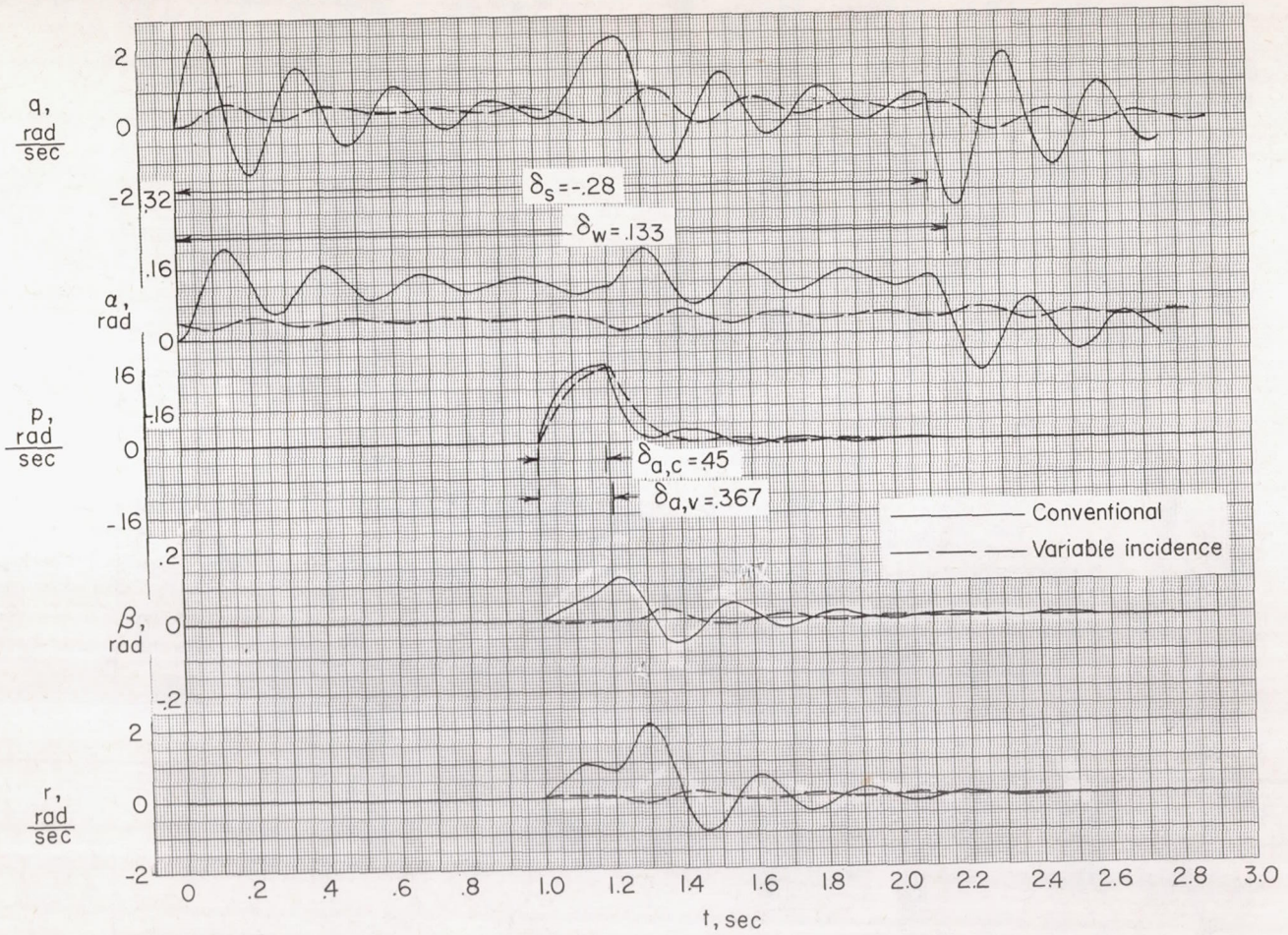

(b) $\delta_{a,c} = 0.450$; $\delta_{a,v} = 0.367$.

Figure 6.- Concluded.

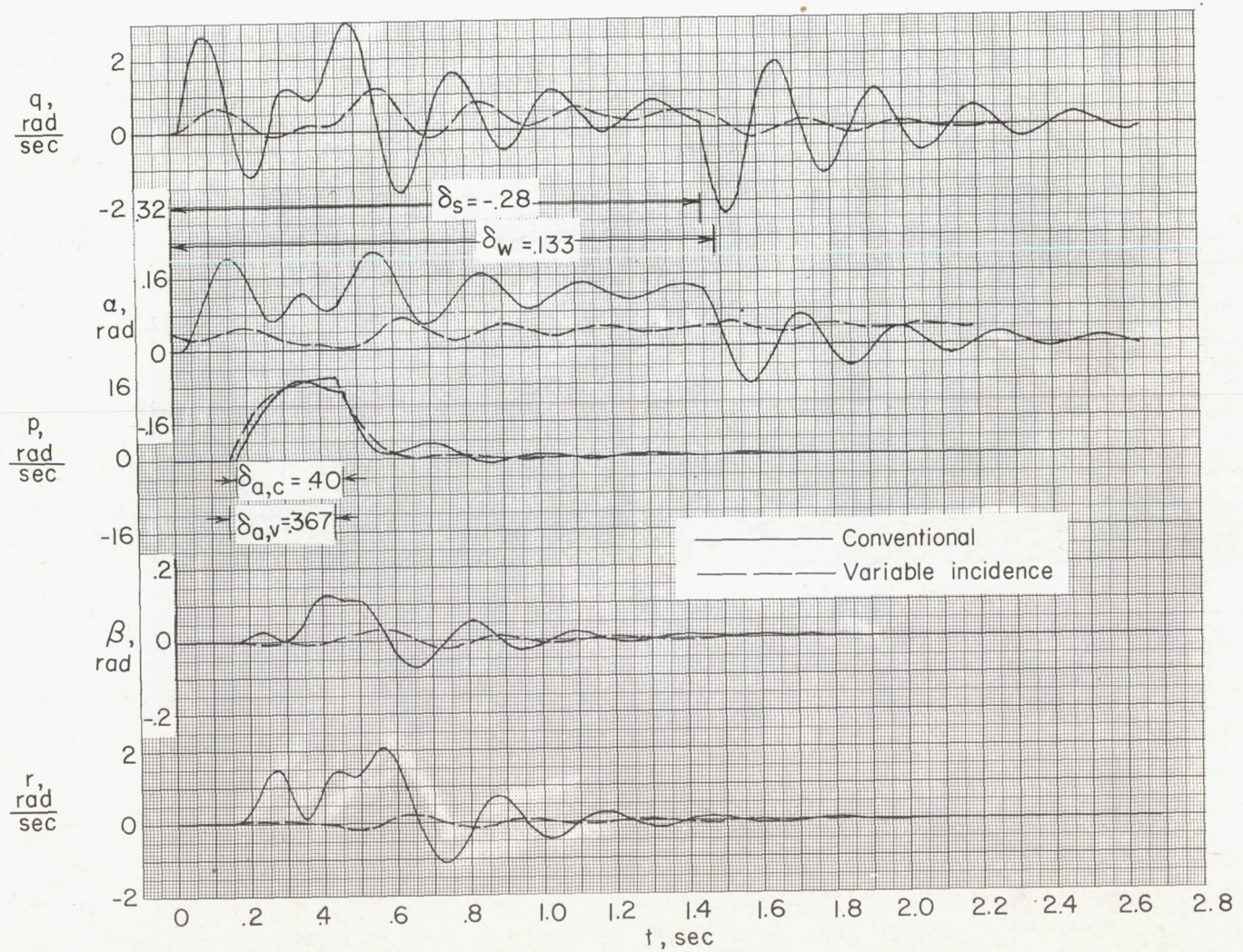

Figure 7.- Combined lateral and longitudinal motions. Aileron deflection applied after one-fourth cycle of pitch oscillation. C_{l_β} = -0.02; $\delta_{a,c}$ = 0.400; $\delta_{a,v}$ = 0.367.

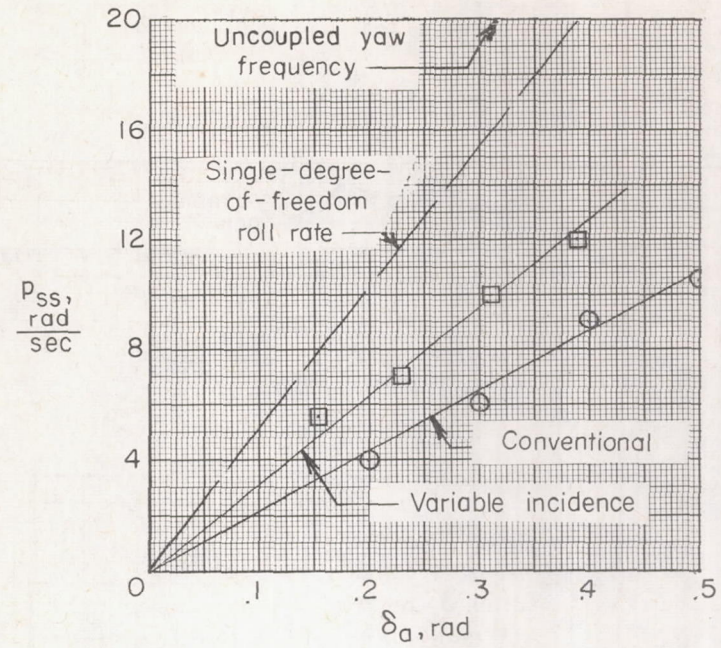

(a) $C_{l_\beta} = -0.10$.

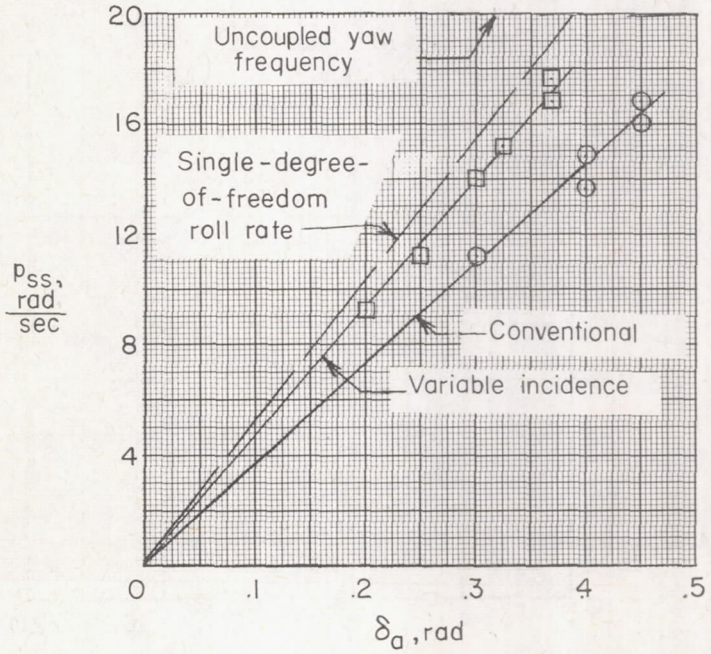

(b) $C_{l_\beta} = -0.02$.

Figure 8.- Approximate steady-state rolling velocities.

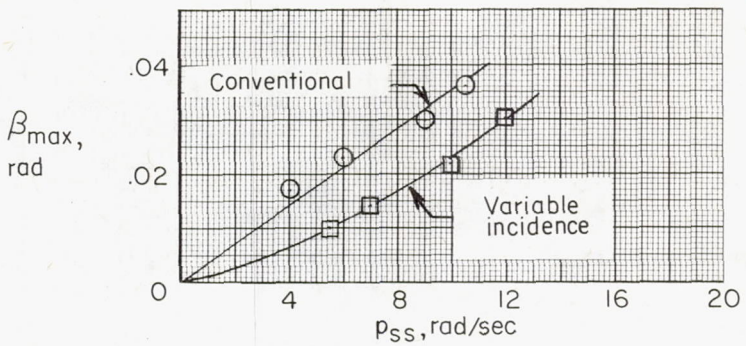

(a) $C_{l_\beta} = -0.10$.

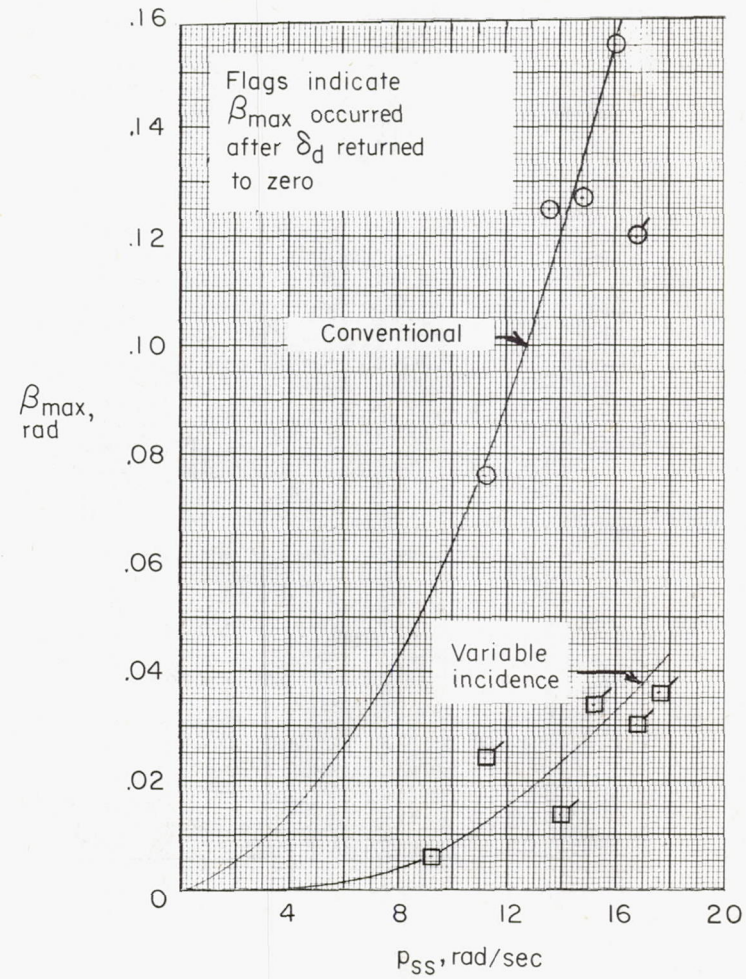

(b) $C_{l_\beta} = -0.02$.

Figure 9.- Maximum sideslip angles obtained during rolling maneuvers.

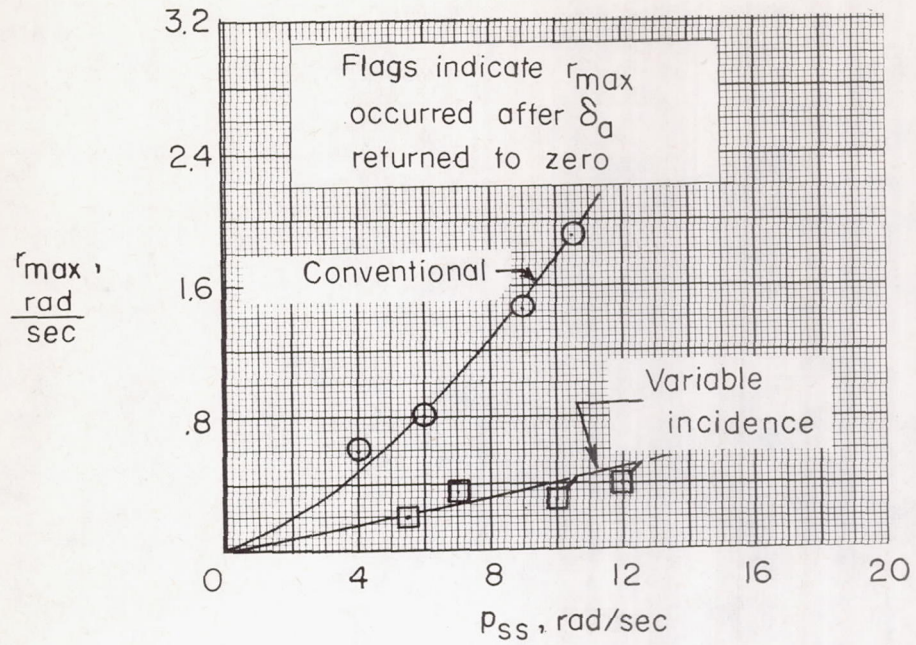

(a) $C_{l_\beta} = -0.10$.

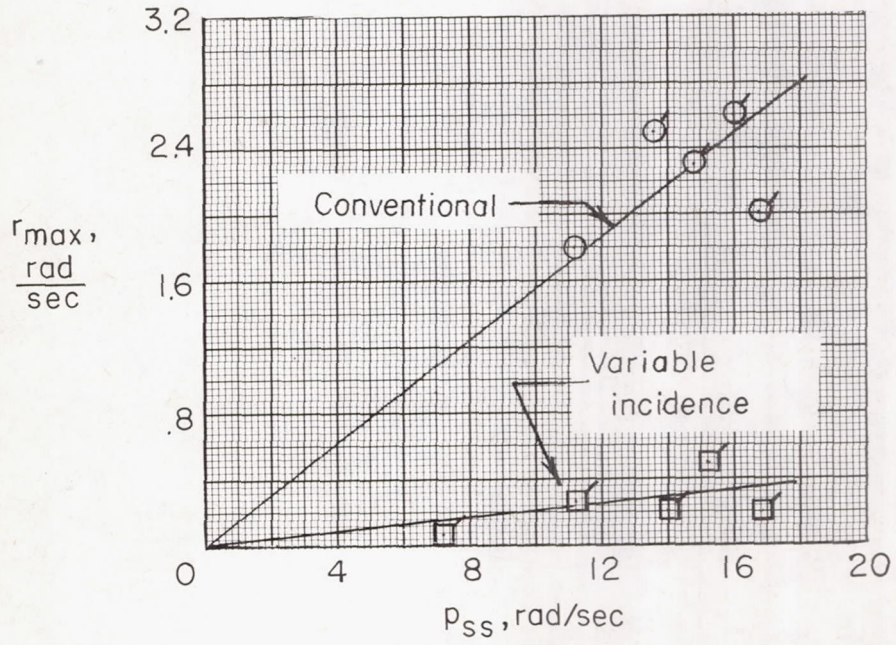

(b) $C_{l_\beta} = -0.02$.

Figure 10.- Maximum yawing velocities obtained during rolling maneuvers.